

## Biophysical characterization of human serum albumin interaction with dapagliflozin: multi-spectroscopic and molecular docking study

Tuvshinjargal Duurenjargal<sup>1,2</sup>, Tuguldur Badamkhatan<sup>2</sup>, Khurelbaatar Luvsanbat<sup>1</sup>,  
Mishig-Ochir Tsogbadrakh<sup>1</sup> and Urnukhsaikhan Enerelt<sup>1\*</sup>

<sup>1</sup> Department of Biology, School of Arts and Sciences,  
National University of Mongolia, Ulaanbaatar, Mongolia

<sup>2</sup> Radiation biophysics laboratory, Institute of Physics and Technology,  
Mongolian Academy of Sciences, Ulaanbaatar, Mongolia

ARTICLE INFO: Received: 12 Dec, 2024; ccepted: 31 Mar, 2025

**Abstract:** Human serum albumin (HSA) is the most abundant protein in human blood plasma and plays a crucial role in drug transport and pharmacokinetics. Dapagliflozin (DAPA), a sodium-glucose co-transporter 2 (SGLT2) inhibitor, is widely prescribed for the treatment of type 2 diabetes mellitus. In the present study, we employed a combination of multi-spectroscopic techniques, including fluorescence spectroscopy (three-dimensional, synchronous), UV-visible absorption spectroscopy, thermodynamic analysis, and molecular docking to investigate the interaction of dapagliflozin with HSA under physiological condition. The quenching mechanism of DAPA was determined to be dynamic through Stern-Volmer and modified Stern-Volmer analyses. The binding constants at 298 K, 303 K, 308 K were  $0.52 \times 10^4$ ,  $0.303 \times 10^4$  and  $0.264 \times 10^4 \text{ M}^{-1}$ , respectively. Thermodynamic analysis revealed that the binding process is spontaneous, driven primarily by hydrogen bonding and hydrophobic interactions at various temperatures. Synchronous fluorescence studies suggest that DAPA binding does not significantly alter the microenvironment around the tyrosine and tryptophan residues of HSA, implying that the binding sites are spatially distinct from these residues. Three-dimensional fluorescence studies reveal that the addition of DAPA to HSA affects changes in the micro-environment and conformation of HSA. UV-VIS spectroscopy confirmed the formation of the HSA-DAPA complex, characterized by spectral shifts in both peptide bond and aromatic amino acid regions, indicating alterations in the protein's secondary structure. The decrease in zeta potential upon DAPA binding suggests a change in the surface charge and potential conformational changes in HSA, which may influence its biological activity and interaction with other molecules. Molecular docking studies identified key amino acid residues involved in the binding of DAPA to HSA, primarily through hydrophobic and hydrogen bond interactions.

**Keywords:** Dapagliflozin, human serum albumin, multi-spectroscopy, zeta-potential, molecular docking;

\*Corresponding author, email: [enerelt@num.edu.mn](mailto:enerelt@num.edu.mn)

<https://orcid.org/0000-0003-4484-4267>



The Author(s). 2025 Open access This article is distributed under the terms of the Creative Commons Attribution 4.0 International License (<https://creativecommons.org/licenses/by/4.0/>), which permits unrestricted use, distribution, and reproduction in any medium, provided you give appropriate credit to the original author(s) and the source, provide a link to the Creative Commons license, and indicate if changes were made.

## INTRODUCTION

Diabetes mellitus is a medical condition characterized by uncontrolled blood glucose levels, excessive urine production by the kidneys, and is caused by chronic high blood sugar levels, as well as either a complete or partial inability of the body to secrete insulin or properly respond to its effects. The two primary classifications of diabetes are known as type 1 diabetes (insulin-dependent diabetes) and type 2 diabetes (non-insulin-dependent diabetes) (1). According to the International Diabetes Federation, approximately 536.6 million adults (10.5%) were estimated to have had Type 2 Diabetes in 2021.

It is projected that the global number of people with diabetes will increase to 783.2 million (12.2%) by the year 2045 (2).

Dapagliflozin (DAPA) classified as a sodium-glucose cotransporter-2 (SGLT2) inhibitor is an oral medication primarily employed for managing type 2 diabetes mellitus (3). Its mode of action revolves around selectively targeting the SGLT2 protein located in the kidneys, which is responsible for the reabsorption of more than 90% of the filtered glucose from the first (S1) and second (S2) segments of the proximal tubule (4).

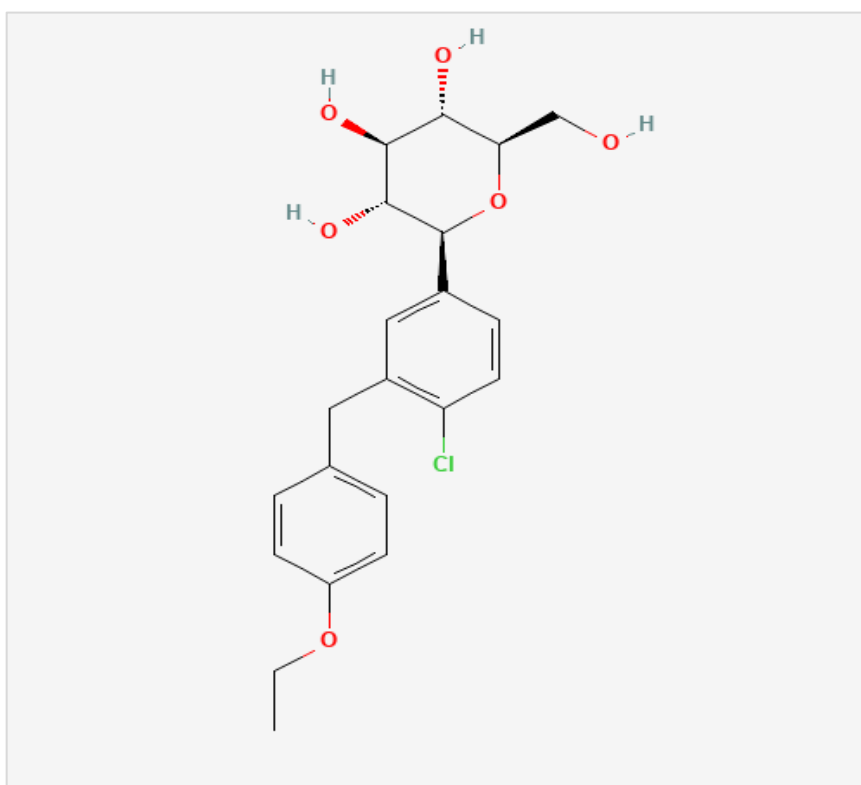


**Figure 1. The chemical structure of dapagliflozin.**

Among the most vital bioactive molecules, proteins are intricately associated with nutrition, immunity, and metabolism, exerting multifaceted roles. In addition to their aforementioned functions, serum proteins actively participate in drug transport, exerting a significant influence over drug absorption, distribution, metabolism and excretion (ADME) (5).

In recent years, Human Serum Albumin (HSA) has been extensively

studied and widely used as a model protein in biophysics, biochemistry, and pharmacology (6). HSA is a protein consisting of a single polypeptide chain of 585 amino acids and has a structure that includes three similar domains. Each domain encompasses two sub-domains (IA, IB, IIA, IIB, IIIA, and IIIB), all of which possess exceptional binding ability with endogenous and exogenous molecules, including small drug compounds (7).

Comprehensive analysis utilizing X-ray crystallography has confirmed that numerous drug molecules specifically bind two distinct drug binding sites on HSA, referred to as the warfarin binding site (site I) and the benzodiazepine binding site (site II), as initially discovered by Sudlow et al. and subsequently validated by Bos et al. These binding sites, known as Sudlow sites, have significance for drug interactions (8,9).

Moreover, the fluorescence emission of HSA predominantly arises from the tryptophan (Trp) amino acid residue situated within the hydrophobic binding pocket of sub-domain IIA (10). Tryptophan residues are strategically located within binding sites of HSA, enabling the molecule to interact with and transport a diverse range of ligands (11). The unique physicochemical properties of tryptophan, such as its aromaticity and hydrophobicity, contribute to the binding affinity and specificity of HSA for different ligands. Therefore, the fluorescence of tryptophan residues in HSA can be useful for studying protein folding, ligand binding, and conformational changes in HSA (12).

Considering the possibility of drug-drug interactions involving HSA, it is essential to understand how dapagliflozin binds to HSA, including its binding affinity and specificity, to evaluate the potential risks of adverse effects when co-administered with other medications.

In 2021, the study of the interaction between dapagliflozin and Bovine Serum Albumin was published by Mohamed A. Abdelaziz et al (13). In Mohamed A. Abdelaziz et al.'s study, the Dapagliflozin and bovine serum albumin interaction study was investigated by spectroscopic and computational methods, e.g. two and three-dimensional fluorescence, synchronous fluorescence, UV-Vis spectrophotometer, FTIR, molecular docking, molecular dynamic simulation, FRET, and binding site determination. Also, Asma Mohamady et.al and Attarat Pattanawongsa et.al studied its drug-drug interaction and glycated human

serum albumin interaction in 2015 and 2021, respectively (14,15)

However, a detailed mechanistic understanding of its interaction with human serum albumin remains elusive, particularly at the molecular level. There are currently no published studies investigating the interaction between dapagliflozin and human serum albumin by multi-spectroscopic analysis, e.g., emission spectroscopy (synchronous and three-dimensional (3D) fluorescence spectroscopy), UV-Vis absorption spectroscopy, and zeta-potentials under physiological conditions and molecular docking method.

## MATERIALS AND METHODS

**Materials:** Human serum albumin (Fatty acid and globulin free, purify >99%) was purchased from Sigma Chemical Co. Dapagliflozin was obtained from AstraZeneca (Mount Vernon, Indiana, USA). All of the other chemicals were used as supplied without further purification. The test tubes were purchased from Padaman LLC (China).

The HSA was prepared by weighing and dissolving the protein in phosphate buffer. (10 mM, pH 7.4). Dapagliflozin solution was prepared by dissolving in organic solution ethanol (12 mM). All reagents were dissolved in ultrapure water and used throughout the experiments. Stock solutions were stored in the dark at 277 K.

## Methods

### Preparation of solutions

A potassium phosphate buffer solution was prepared at a concentration of 0.01 mmol/L and its pH was adjusted to 7.4 with a 1 M NaOH solution. The HSA stock solution was prepared at 2  $\mu$ M in phosphate buffer, and 5 mmol/L stock of DAPA was prepared in methanol. UV-vis absorbance, synchronous fluorescence, three-dimensional spectroscopy, and zeta potential of HSA and DAPA were recorded, and spectral measurements were obtained

under the same condition. All experiments were recorded at pH 7.4.

## Apparatus and Methods

### Fluorescence Spectra Measurements

The fluorescence spectra measurements were performed on a Hitachi F-4600 spectrofluorometer (Tokyo, Japan) with a xenon lamp and 1cm quartz cell and thermoblock (Daihan Scientific Co., Ltd). The excitation wavelength was set at 280 nm, and the emission was measured from 300-500 nm at each temperature (298 K, 303 K, 308 K). The excitation and emission bandwidths were set at 5nm. The response time and the scan speed were fixed at 700 V, 1.0 s, and 1200 nm min<sup>-1</sup> respectively. 2 µM HSA was titrated with increasing concentrations of DAPA (1-50 µM) in 0.01 mmol/L potassium phosphate buffer at pH 7.4, and the fluorescence spectra were recorded.

### Synchronous and Three-dimensional Fluorescence Spectra Measurements

Synchronous and three-dimensional fluorescence measurements were carried out in Hitachi F-4600 spectrofluorometer (Tokyo, Japan). Synchronous fluorescence spectra were recorded in the wavelength range from 200-500 nm at 298 K. The scanning wavelength interval ( $\Delta\lambda = \lambda_{ex} - \lambda_{em}$ ) was  $\Delta\lambda = 15$  nm,  $\Delta\lambda = 60$  nm, which were used for properties of tyrosine and tryptophan residues of HSA, respectively. 2 µM HSA was titrated with increasing concentrations of DAPA (1-50 µM) in 0.01 mmol/L potassium phosphate buffer at pH 7.4, and the synchronous fluorescence spectra were recorded.

Three-dimensional fluorescence spectra for the HSA-DAPA complex system were performed in the presence and absence of 50 µM DAPA at the excitation wavelength range from 200 to 340 nm and the emission wavelength from 200 to 500 nm at 298K.

### UV-visible spectra measurements

All UV-Vis absorption spectra measurements were taken using a UV-VisM51 spectrophotometer (Berlin, Germany) with 1cm quartz cell at room temperature. UV-Vis absorption spectra of HSA (2 µM) were measured in the wavelength range between 200–500 nm by titrating the concentration of DAPA drug (10-50 µM).

### Zeta potential measurement

Zeta potential measurement was carried out using a Zeta-potential analyzer - ZetaCad instrument (Paris, France) with Zeta compact 6.0 software.

The surface charge of HSA was measured using the Zeta potential meter, and the total volume of the solution was calculated as 15 ml. Human serum albumin and Dapagliflozin concentrations for  $\zeta$ -potential analysis were selected to get the same molar ratio like for fluorescence studies.

### Molecular docking

Molecular docking simulations were conducted to predict the binding affinity and mode of interaction between DAPA and sites I and II of HSA, using AutoDock Vina 1.1.2, AutoDockTools 1.5.7. The crystal structure of HSA (PDB ID: 1AO6) was prepared by removing all water molecules to maintain its 3D structure. And the ligand, Dapagliflozin 3D structure was downloaded from ChEMBL (ID: 429910) and converted to pdbqt file using Openbabel. The ligand DAPA was constrained to have 12 degrees of torsional freedom due to the flexible bonding. Only polar hydrogen atoms were added to both DAPA and HSA molecules.

Kollman partial charges were subsequently assigned to all atoms. A 100x100x100 Å grid was generated with a spatial resolution of 0.375 Å. The central coordinates of the grid cell were set to x-24.515, y-33.299, and z-37.252. A docking analysis was then performed with 10000 iterations centered on this grid. The complex formed between DAPA and HSA was visualized using UCSF Chimera 1.16 and PyMol software.

## RESULTS AND DISCUSSION

## Fluorescence study of HSA-DAPA system

Molecular fluorescence quenching is a sensitive technique used in biophysical research to study drug interactions with human serum albumin. This method is valuable for drug discovery, development, pharmacokinetics, pharmacodynamics, energy transfer, and binding affinity of drugs(16). Fluorescence quenching occurs through two main mechanisms: static and dynamic quenching. Static quenching involves the formation of a complex between the drug and HSA, while dynamic quenching results from collisions between the excited-state drug and HSA. Factors like temperature, pH, ionic strength, and drug concentration influence the extent of quenching and the binding properties of the HSA-drug complex. The intrinsic fluorescence of albumin, primarily due to tryptophan residues, is sensitive to changes in its microenvironment. Binding of small molecules to albumin alters this microenvironment, leading to changes in

fluorescence intensity, a phenomenon underlying the quenching process(17).

HSA has the highest fluorescence emission at 353 nm at excitation wavelength  $\lambda=280$ . The decrease of fluorescence intensity of HSA has been monitored at 353 nm for HSA-DAPA system (Figure 2A). As the concentration of the quencher molecule increased, the shape of the spectra remained unchanged, but a slight blue shift of approximately 5 nm was observed. This result indicates the formation of a complex between HSA-DAPA.

The concentration-dependent decrease in HSA fluorescence intensity upon DAPA binding indicates there is an interaction. The observed blue shift in the maximum emission wavelength suggests that the tryptophan residue of HSA is moving to a more hydrophobic environment upon complex formation.

We applied the Stern-Volmer equation (1) to study fluorescence quenching by varying complex concentration at different temperatures:

$$F_0/F = 1 + K_q\tau_0 = 1 + K_{sv}[Q] \quad (1)$$

Where  $F_0$  and  $F$  represent fluorescence intensities of HSA in the absence and presence of DAPA quencher molecule, respectively.  $F_0$  is the fluorescence intensity of HSA. The biomolecular quenching rate constant is denoted as  $K_q$ , the average lifetime of the

biomolecule without quencher is represented as  $\tau_0$ , and  $Q$  indicates the concentration of the DAPA. Biopolymer lifetime is  $10^{-8}$  s for HSA and BSA. The constant of the quenching rate is found by the following equation:

$$K_q = K_{sv} / \tau_0 \quad (2)$$

The values of the Stern-Volmer constant ( $K_{sv}$ ) and dynamic, static quenching both distinguished by the quenching rate constant ( $K_q$ ) of the HSA-DAPA interaction at different temperatures

are calculated according to the formula shown in (1), and results are shown in Table 1. The constant of the Stern-Volmeris increased with increasing temperature, which indicates that the quenching process is dynamic (18).

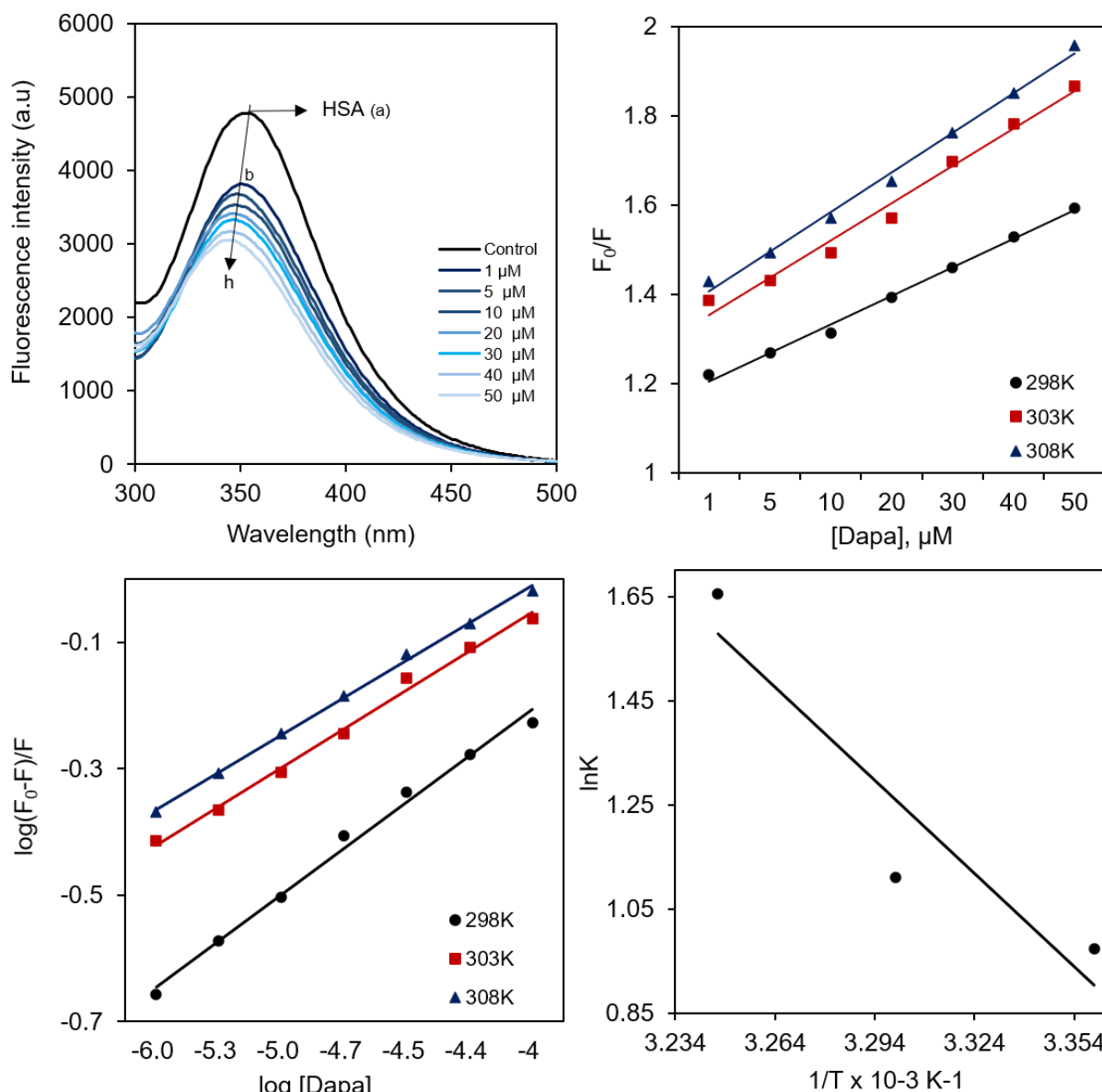


**Figure 2. (A) Fluorescence spectra of HSA-DAPA system. (a)  $2 \times 10^{-6}$  mol/L HSA, (b-h) HSA in the presence of  $10^{-6}$ ,  $5 \times 10^{-6}$ ,  $10 \times 10^{-6}$ ,  $20 \times 10^{-6}$ ,  $30 \times 10^{-6}$ ,  $40 \times 10^{-6}$ ,  $50 \times 10^{-6}$  mol/L DAPA, pH 7.4, T = 298 K. (B) Stern-Volmer plot of HSA quenching for various DAPA concentration at different temperatures. (C) Double logarithmic plot for the quenching of HSA by DAPA at different temperatures. (D) Van't Hoff plot for the interaction of HSA and DAPA.**

**Table 1. Stern-Volmer and quenching rate constant of HSA-DAPA complex at different temperatures.**

| pH  | Temperature (K) | $K_{sv}$<br>( $\times 10^4 \text{ M}^{-1}$ ) | $K_q$<br>( $\times 10^{12} \text{ M}^{-1} \text{ s}^{-1}$ ) | $R^2$  |
|-----|-----------------|--|---|--------|
| 7.4 | 298             | 6.39   | 6.39  | 0.9938 |
|     | 303             | 8.38   | 8.38  | 0.9843 |
|     | 308             | 8.92   | 8.92  | 0.9943 |

$R^2$  – correlation coefficient.

**Thermodynamics and binding forces**

Non-covalent interactions between molecules and macromolecules are primarily hydrogen bonding, electrostatic, van der Waals, and hydrophobic forces. According to the modified Stern-Volmer equation, it is possible to calculate the

$$\text{Log} \left( \frac{F_0 - F}{F} \right) = \text{Log} K_a + n \text{Log} [Q] \quad (3)$$

Here  $F_0$ ,  $F$  are the fluorescence intensities of the HSA with or without the addition of the quencher molecule;  $K_a$ -

binding constant ( $K_a$ ) and the number of binding sites ( $n$ ) of the HSA-DAPA complex (13). Modified Stern-Volmer equation:

binding constant; number of DAPA binding sites ( $n$ ) on HSA;  $[Q]$  is the concentration of the quencher molecule.

**Table 2. Binding and thermodynamic parameters of HSA-DAPA antidiabetic drug complex at different temperatures.**

| pH  | T (K) | $K_a (\times 10^4 \text{ M}^{-1})$ | $n$  | $R^2$  | $\Delta G^\circ$<br>(kJ mol <sup>-1</sup> ) | $\Delta S^\circ$<br>(J mol <sup>-1</sup> K <sup>-1</sup> ) | $\Delta H^\circ$<br>(kJ mol <sup>-1</sup> ) |
|-----|-------|------------------------------------|------|--------|---|--|---|
| 7.4 | 298   | 0.523                              | 0.73 | 0.9979 | -75.60                                      | 3.137  | 2.841                                       |
|     | 303   | 0.303                              | 0.61 | 0.9934 | -91.3                                       |  |   |
|     | 308   | 0.264                              | 0.58 | 0.992  | -106.99                                     |  |   |

$R^2$ -correlation coefficient

The fluorescence quenching behavior of the protein was investigated to elucidate the quenching mechanism and rates. Stern-Volmer analysis was performed on the relative fluorescence intensity  $F_0/F$  as a function of quencher concentration  $[Q]$ . Figure 2B shows Stern-Volmer plot at 298 K, 303 K, and 308 K. The number of binding sites and binding constant can be determined by  $\log [(F_0-F)/F]$  versus  $\log [Q]$

based on equation (3) (13). Experiments indicate that the binding constants ( $K_a$ ) $\times 10^4 \text{ M}^{-1}$  of the HSA-DAPA system at various temperatures shows moderate binding. The thermodynamic parameters  $\Delta G^\circ$ ,  $\Delta H^\circ$ ,  $\Delta S^\circ$ , which control the interaction of HSA and DAPA, are collected in Table 2 and were obtained using the Van't Hoff equation (4) and the Gibbs free energy equation (5):

$$\ln K_A = \frac{-\Delta H}{RT} - \frac{\Delta S}{RT} \quad (4)$$

Here  $R$  is the gas constant (8.314 J. mol<sup>-1</sup> K<sup>-1</sup>);  $T$ -temperature (298 K, 303 K, 308 K);  $K_A$ - Modified Stern-Volmer binding constant depending to each temperature.

The Gibbs free energy is calculated by the following formula:

$$\Delta G^0 = \Delta H^0 - T \Delta S^0 \quad (5)$$

To calculate the thermodynamic parameters of the drug interaction HSA-DAPA, we took a natural logarithm of values of the protein-drug binding constant and temperature-dependent Van't Hoff plot (Figure 2 C).

The values of the thermodynamics and binding constants are shown in Table 2. In our experiments, the enthalpy changes ( $\Delta H$ ) and entropy changes ( $\Delta S$ ) were greater than zero, indicating that the drug was bound to the hydrophobic part of the protein and that

the Gibbs free ( $\Delta G$ ) energy changes were negative, indicating that the HSA-DAPA process was spontaneous (19)

### Synchronous fluorescence spectroscopy study

Our study demonstrates that the binding of DAPA to HSA causes fluorescence quenching. However, the potential impact of this binding on the conformation and/or molecular environment surrounding HSA remains uncertain. Synchronous fluorescence spectroscopy, a sensitive and selective technique, further investigated DAPA-HSA binding (20).

Synchronous fluorescence spectra (SFS) indicate ligand-induced changes in

the microenvironment of tyrosine and tryptophan residues in human serum albumin (21). By simultaneously scanning excitation and emission monochromators at a fixed wavelength interval ( $\Delta\lambda$ ), synchronous fluorescence spectroscopy (SFS) provides specific information on tyrosine ( $\Delta\lambda = 15$  nm) and tryptophan ( $\Delta\lambda = 60$  nm) residues in HSA. Figure 3 shows the synchronous fluorescence spectrum of HSA as a function of DAPA drug concentration. There was no peak shift in the spectra of tryptophan ( $\Delta\lambda = 60$  nm) and tyrosine ( $\Delta\lambda = 15$  nm). These findings indicate that the microenvironments of tryptophan and tyrosine remain unaltered upon DAPA binding to HSA, suggesting that these amino acid residues are spatially distant from the binding site (22).

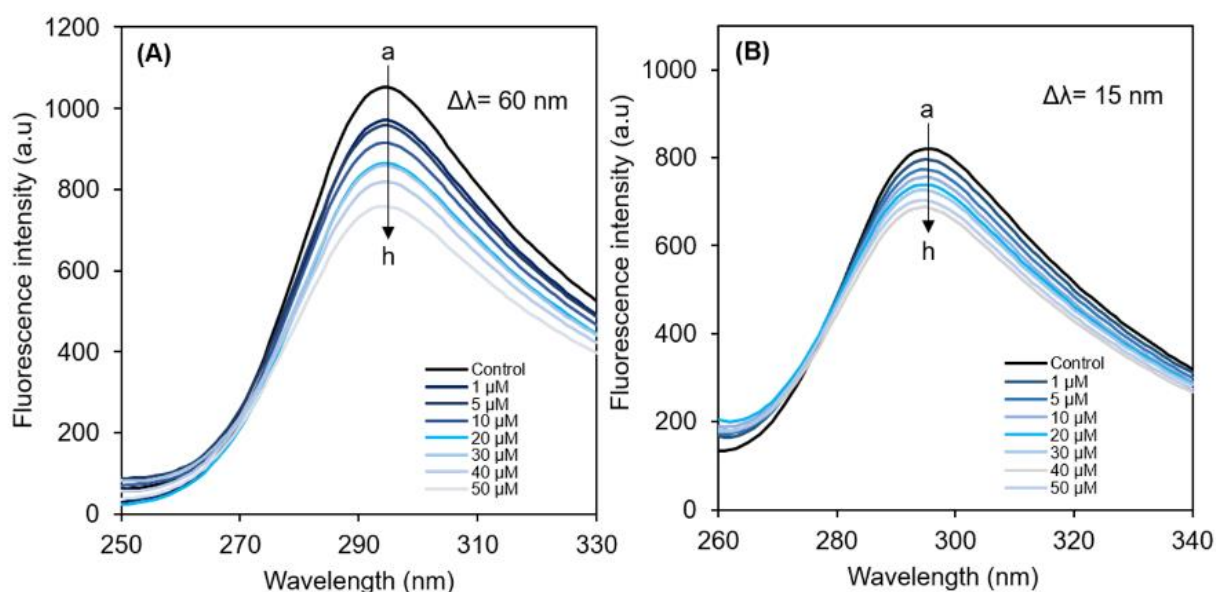


**Figure 3.** Synchronous fluorescence spectra of (A) tyrosine ( $\Delta\lambda = 15$  nm) and (B) tryptophan ( $\Delta\lambda = 60$  nm). (a)  $2 \times 10^{-6}$  mol/L HSA, (b-h) HSA in the presence of  $10^{-6}$ ,  $5 \times 10^{-6}$ ,  $10 \times 10^{-6}$ ,  $20 \times 10^{-6}$ ,  $30 \times 10^{-6}$ ,  $40 \times 10^{-6}$ ,  $50 \times 10^{-6}$  mol/L DAPA, pH 7.4,  $T = 298$  K.

### Three-dimensional fluorescence spectroscopy

Three-dimensional fluorescence spectroscopy was used in addition to quenching and synchronous fluorescence to study the HSA-DAPA complex. Three-dimensional fluorescence spectroscopy is a

comprehensive luminescence technique that simultaneously measures the excitation, emission, and intensity wavelengths of complex fluorophores. It can provide detailed insights into structural changes within the polypeptide backbone and alterations in the polarity of the microenvironment surrounding tryptophan

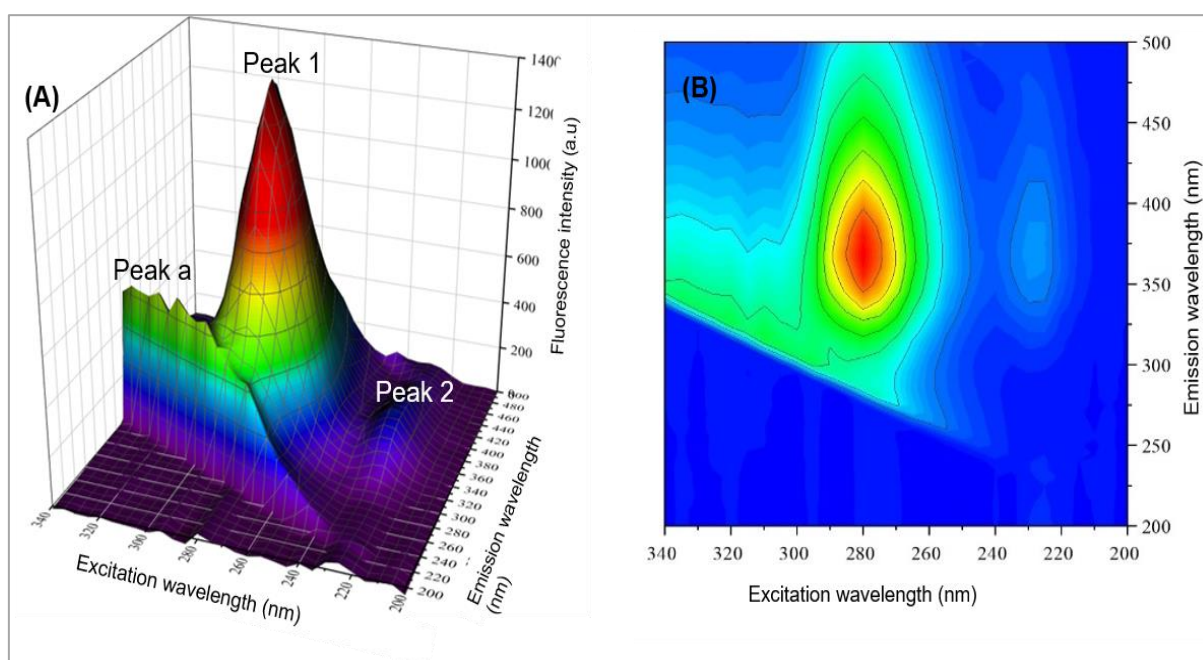
and tyrosine residues, induced by ligand binding (23). 3D spectra can reveal conformational changes in HSA, such as wavelength shifts, new peak formation, or peak disappearance (24). The 3D spectra and the contour spectra of HSA and the HSA-DAPA complex system are shown in Figures 4 and 5, respectively. There are three peaks of free HSA that are generally detected in the 3D fluorescence spectrum. The corresponding 3D fluorescence spectrum data are listed in Table 3.

As shown in Figures 4 and 5, peak “a” represents the Rayleigh scattering peak ( $\lambda_{em} = \lambda_{ex}$ ). At the same time, there are two typical fluorescence peaks observed in 3D fluorescence spectra. Peak 1 ( $\lambda_{ex}=280$  nm,  $\lambda_{em}=370$  nm) mainly revealed the spectral feature of Trp and Tyr residues, and peak 2 ( $\lambda_{ex}=230$  nm,  $\lambda_{em}=375$  nm) displays fluorescence behavior of the polypeptide

of  $\pi \rightarrow n^*$  of C=O group in HSA, and its intensity is related to the secondary structure of the protein (25).

Upon the addition of DAPA, a blue shift of 10 nm was observed for peak 1 (from  $\lambda_{ex}/\lambda_{em} = 280/370$  nm to  $\lambda_{ex}/\lambda_{em} = 280/360$  nm) and an 8 nm blue shift for peak 2 (from  $\lambda_{ex}/\lambda_{em} = 230/375$  nm to  $\lambda_{ex}/\lambda_{em} = 230/367$  nm). These spectral shifts indicate a decrease in the polarity and an increase in the hydrophobicity of the tryptophan microenvironment, suggesting a conformational change in the HSA structure.

Changes in the Rayleigh scattering peak intensity upon DAPA binding suggest alterations in the surface properties of the HSA. The observed decrease in scattering intensity with increasing DAPA concentration indicates a reduction in HSA's size and a change in its



backbone, which is caused by the transition

microenvironment.

**Figure 4. 3D fluorescence spectra of HSA (A) and its contour spectra (B) [HSA] =  $2 \times 10^{-6}$  M, pH 7.4, T = 298 K.**

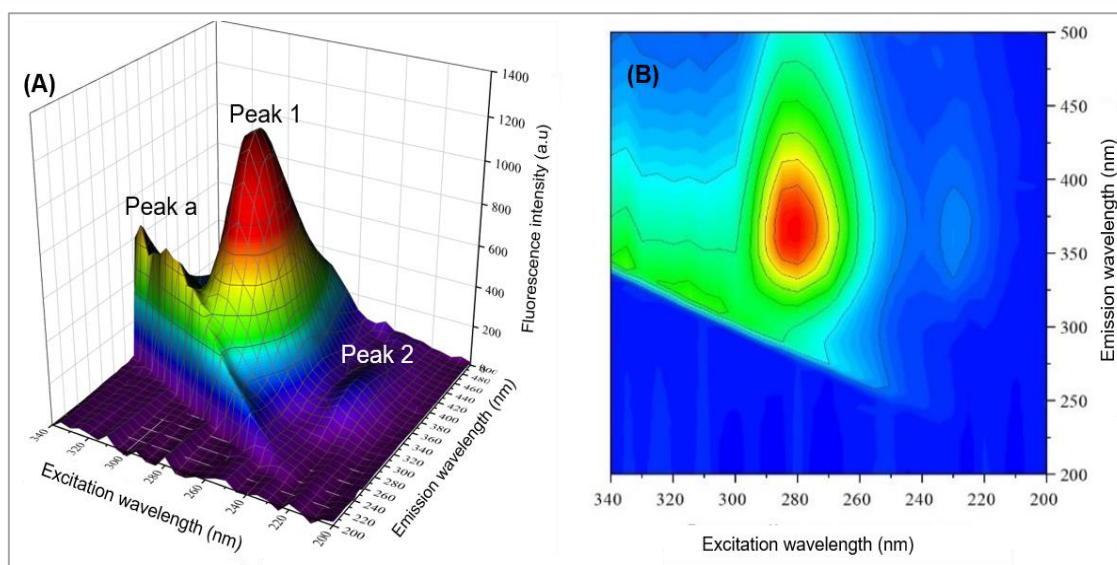


**Figure 5. 3D fluorescence spectra of HSA-DAPA system (A) and its contour spectra (B) [HSA] =  $2 \times 10^{-6}$  M, [DAPA] =  $50 \times 10^{-6}$  M, pH 7.4, T = 298 K.**

**Table 3. 3D fluorescence spectra parameter for HSA and HSA-DAPA system.**

|                            |        | HSA                                    |               | HSA-DAPA system                        |               |
|----------------------------|--------|--|---------------|--|---------------|
| Peaks                      |        | Peak position                          | Intensity (F) | Peak position                          | Intensity (F) |
|                            |        | $\lambda_{ex}/\lambda_{em}$<br>(nm/nm) |               | $\lambda_{ex}/\lambda_{em}$<br>(nm/nm) |               |
| Fluorescence peak          | Peak 1 | 280/370                                | 1417          | 280/360                                | 1196          |
|                            | Peak 2 | 230/375                                | 189.8         | 230/367                                | 149.7         |
| Rayleigh scattering peak a |        | 280/280                                | 430.2         | 280/280                                | 334.4         |

#### UV-Visible absorption spectral study

Investigating protein conformational changes can be effectively accomplished using UV-vis absorption spectroscopy, which is a straightforward yet powerful technique. Confirmation changes caused by ligands in the protein's absorption spectrum are generally shown as evidence of the formation of a complex between the ligand and the protein. Additionally, UV-Vis spectral analysis has been utilized to enhance the understanding of how ligands induce the quenching of protein fluorescence (26),(27).

We measured the UV-vis absorption

spectra of HSA in the absence and presence of DAPA, which is presented in Figure 6. As the concentration of DAPA drug increased, the absorption intensity increased as well. The HSA-DAPA complex measured by UV-Vis had two characteristic peaks, and due to the formation of the HSA-DAPA drug complex, there was one strong peak around 205 nm and red shift from  $\lambda_{max}$ -205 nm to  $\lambda_{max}$ -209 nm in the short wavelength range. There was a peak at 278 nm and it shifted blue from  $\lambda_{max}$ -278 nm to  $\lambda_{max}$ -275 nm (aromatic amino acid residue).

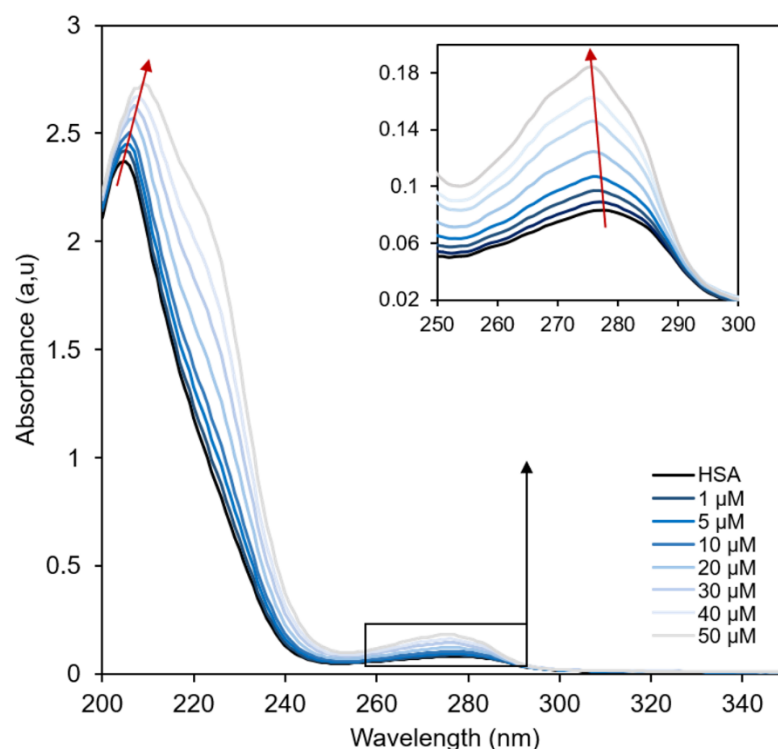


**Figure 6.** UV-Vis absorption spectra of HSA in the presence of DAPA,  $[HSA] = 2 \times 10^{-6} \text{ M}$ ,  $[DAPA] = (0-50) \times 10^{-6} \text{ M}$ , pH 7.4,  $T = 298 \text{ K}$ .

These results show that the binding of DAPA led to peptide bonds conformational changes in HSA of absence and presence of DAPA.

### Zeta Potential analysis

The zeta potential, denoting the surface charge characteristic of a biomacromolecule like HSA in solution, is influenced by physiological pH conditions, such as pH 7.4 (28). The protein surface charge is related to its amino acid's ionization (29). The negative charge exhibited by HSA at pH 7.4 mainly emanates from the carboxyl groups ( $\text{COOH}$ ) positioned within the side chains of amino acids like aspartic acid and glutamic acid. Under these pH circumstances, these carboxyl groups tend to release a proton ( $\text{H}^+$ ), resulting in their transformation into carboxylate ions ( $\text{COO}^-$ ) carrying a negative charge. This interplay significantly contributes to the

overall negative charge of the protein molecule (30).

To authenticate potential drug binding, zeta potential measurements were performed under physiological pH 7.4. This measurement was based on the premise that the protein and drugs possess distinct net electric charges at a specific pH range.

Specifically, the zeta potential value of HSA in the absence of drugs, indicated in Figure 7, was recorded as  $-22.38 \text{ mV}$ . Further examination of Figure 7 revealed a decrease in the zeta potential of the protein upon DAPA binding. When the DAPA concentration increased from  $10\text{--}50 \text{ }\mu\text{M}$ , the zeta-potential slightly decreased from  $-22.38 \text{ mV}$  to  $-34.89 \text{ mV}$ . This phenomenon might be attributed to a potential expansion of the protein's configuration due to elevated drug concentrations and the involvement of hydrophobic interactions during this process.

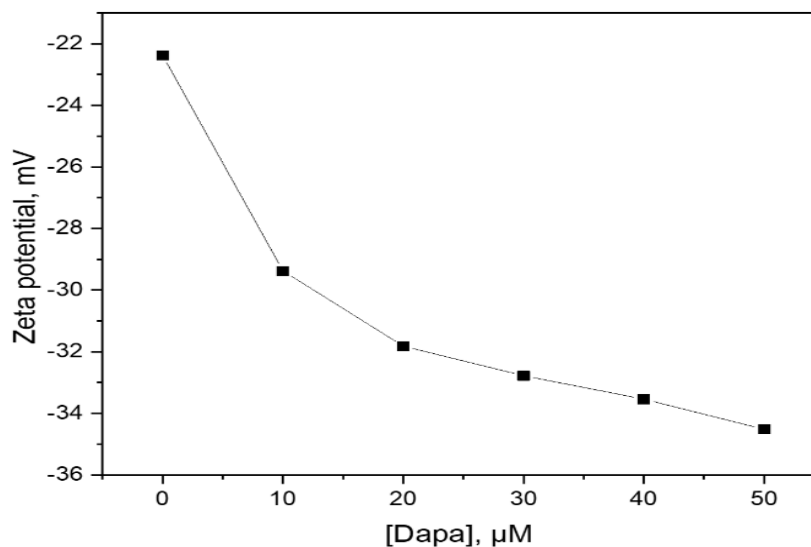


**Figure 7.** Effect of DAPA on the zeta potential of HSA. [HSA] =  $2 \times 10^{-6}$  M, [DAPA] =  $(10-50) \times 10^{-6}$  M, pH 7.4, T = 298 K.

### Molecular docking study

It has become essential in silico methods, such as molecular modelling, to develop new therapeutic agents by examining how small molecules like drugs interact with biological macromolecules such as DNA and proteins (31). A molecular docking study was carried out to identify DAPA's primary binding site on HSA. The binding mode of DAPA to HSA with the lowest energy rate is shown in Figure 8. As can be seen in Figure 8, DAPA molecule is

surrounded by Ala-191, Lys-195, Asp-451, Tyr-452, and Val-455, as well as hydrogen bonds with Arg-218, Asn-295, and Lys-436 with the binding energy of  $-6.37 \text{ kcal/mol}^{-1}$ . Thus, several forces like hydrophobic, hydrogen bonding or  $\pi$ -stacking,  $\pi$ -cation maintain a crucial role in occupancy of the DAPA at relevant site of HSA protein, which might induce some minor modification in conformations of the protein secondary structure. Also, DAPA molecule binds dominantly to Sudlow site II (domain III) of HSA.

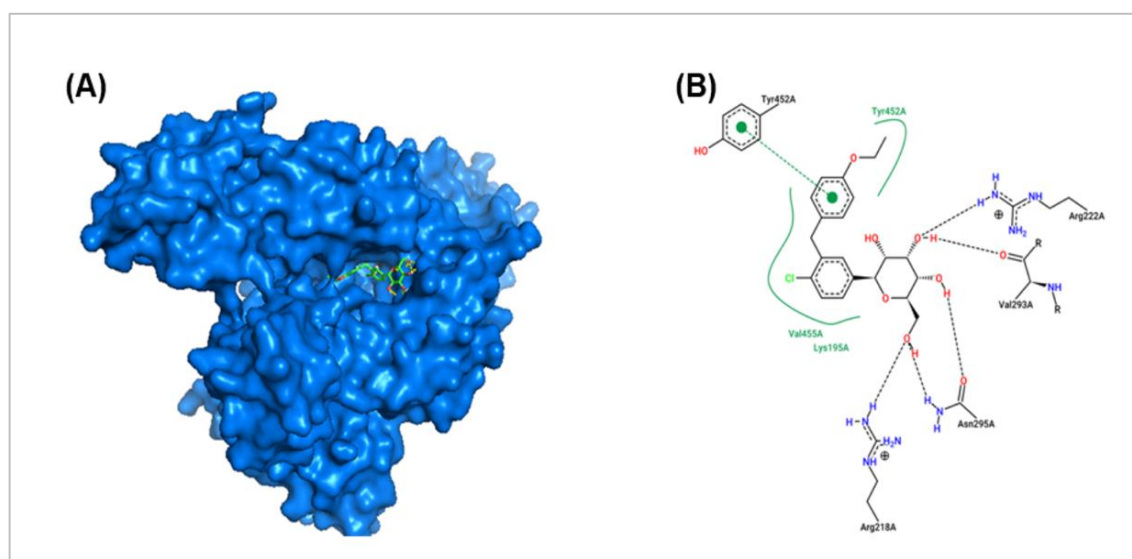


**Figure 8.** (A) Dapagliflozin molecule located in the hydrophobic cavity of human serum albumin. (B) 2D representation of the interaction between HSA and DAPA.

## CONCLUSIONS

In this study, we used multi-spectroscopic methods to explore the interactions between DAPA and HSA under physiological conditions. The experimental results showed that the fluorescence quenching of HSA by antidiabetic for type 2 diabetes drug DAPA was a result of the formation of complex between them by dynamic quenching. DAPA moderately binds to the Sudlow site II of HSA through hydrogen bonds and hydrophobic interactions, as indicated by the Stern-Volmer constant ( $K_{SV}$ ), binding constant ( $K_a$ ), and thermodynamic parameters. The thermodynamic analysis showed that the binding process was endothermic ( $\Delta H^\circ > 0$ ) and spontaneous ( $\Delta G^\circ < 0$ ). Using synchronous and 3D fluorescence spectroscopy, we determined that the interaction between DAPA and HSA resulted in a change in the secondary structure ratio of albumin, leading to a more hydrophobic microenvironment around the tryptophan amino acid residues. Furthermore, the formation of the DAPA-HSA complex resulted in a more negative surface zeta potential of the albumin, which corroborated the findings from synchronous and 3D fluorescence spectroscopy. UV-Vis spectra revealed that the secondary structure of the HSA changed in the presence of DAPA.

This research provides valuable insights into molecular interactions between the DAPA and HSA, suggesting that DAPA binds strongly to HSA, inducing conformational changes that could impact drug delivery and efficacy. This knowledge may contribute to the development of more effective drug delivery strategies and personalized medicine approaches, and further studies are needed to explore the long-term effects of DAPA binding on HSA function and its potential impact on drug metabolism and distribution.

## Acknowledgements

This research work was supported by the Mongolian Foundation for Science and

Technology (Grant No.2022/161) funded by the Mongolian Government.

## Author contribution

The authors confirm contribution to the paper as follows: Study conception and design: UE, M-OTS, TD; data collection: UE, TD; data analysis: UE, TD; molecular docking calculation: KHL; draft manuscript preparation: TD, TB, UE; All authors reviewed the results and approved the final version of the article.

## Conflict of interest

These authors declare that there is no conflict of interest.

## REFERENCES

1. Wu Y, Ding Y, Tanaka Y, Zhang W. Risk factors contributing to type 2 diabetes and recent advances in the treatment and prevention. Vol. 11, International journal of medical sciences. 2014. p. 1185–200.  
<https://doi.org/10.7150/ijms.10001>.
2. Sun H, Saeedi P, Karuranga S, Pinkepank M, Ogurtsova K, Duncan BB, et al. IDF Diabetes Atlas: Global, regional and country-level diabetes prevalence estimates for 2021 and projections for 2045. Diabetes Res Clin Pract. 2022 Jan 1;183.  
<https://doi.org/10.1016/j.diabres.2021.109119>.
3. Shah N. K., Deeb W. E., Choksi R, Epstein B. J. Dapagliflozin: A Novel Sodium-Glucose Cotransporter Type 2 Inhibitor for the Treatment of Type 2 Diabetes Mellitus [Internet]. Available from:  
<https://caesar.sheridan.com/reprints/redir>.  
<https://doi.org/10.1002/PHAR.1010>.
4. List J. F., Whaley J. M. Glucose dynamics and mechanistic implications of SGLT2 inhibitors in animals and humans. Vol. 79, Kidney International.

2011.  
<https://doi.org/10.1038/ki.2010.512>.
5. Dingemanse J, Appel-Dingemanse S. Integrated Pharmacokinetics and Pharmacodynamics in Drug Development. Vol. 46, Clin Pharmacokinet. 2007.  
<https://doi.org/10.2165/00003088-200746090-00001>.
6. Reichenwallner J, Michler S, Schwieger C, Hinderberger D. Human Serum Albumin Loaded with Fatty Acids Reveals Complex Protein-Ligand Thermodynamics and Boleadora-Type Solution Dynamics Leading to Gelation. Journal of Physical Chemistry B. 2025 Apr 10;  
<https://doi.org/10.1021/acs.jpcb.4c08717>.
7. Ashraf S, Qaiser H, Tariq S, Khalid A, Makeen H.A., Alhazmi H.A., et al. Unraveling the versatility of human serum albumin – A comprehensive review of its biological significance and therapeutic potential. Vol. 6, Current Research in Structural Biology. Elsevier B.V.; 2023.  
<https://doi.org/10.1016/j.crstbi.2023.100114>.
8. Yamasaki K, Chuang V. T. G., Maruyama T, Otagiri M. Albumin-drug interaction and its clinical implication. Vol. 1830, Biochimica et Biophysica Acta - General Subjects. Elsevier B.V.; 2013. pp. 5435–43.  
<https://doi.org/10.1016/j.bbagen.2013.05.005>.
9. Lee P, Wu X. Review: Modifications of Human Serum Albumin and Their Binding Effect.  
<https://doi.org/10.2174/1381612821666150302115025>.
10. Ge F, Chen C, Liu D, Han B, Xiong X, Zhao S. Study on the interaction between theasinesin and human serum albumin by fluorescence spectroscopy. J Lumin. 2010 Jan;130(1):168–73.  
<https://doi.org/10.1016/j.jlumin.2009.08.003>.
11. Tayeh N, Rungassamy T, Albani J.R. Fluorescence spectral resolution of tryptophan residues in bovine and human serum albumins. J Pharm Biomed Anal. 2009 Sep 8;50(2):107–16.  
<https://doi.org/10.1016/j.jpba.2009.03.015>.
12. Wang P. Y., Yang C. T., Chu L. K. Differentiating the protein dynamics using fluorescence evolution of tryptophan residue(s): A comparative study of bovine and human serum albumins upon temperature jump. Chem Phys Lett. 2021 Oct 16;781.  
<https://doi.org/10.1016/j.cplett.2021.138998>.
13. Abdelaziz M.A., Shaldam M, El-Domany R.A., Belal F. Multi-Spectroscopic, thermodynamic and molecular dynamic simulation studies for investigation of interaction of dapagliflozin with bovine serum albumin. Spectrochim Acta A Mol Biomol Spectrosc. 2022 Jan 5;264.  
<https://doi.org/10.1016/j.saa.2021.120298>.
14. Pattanawongsa A, Chau N, Rowland A, Miners J. O. Inhibition of human UDP-glucuronosyltransferase enzymes by canagliflozin and dapagliflozin: Implications for drug-drug interactions. Drug Metabolism and Disposition. 2015 Oct 1;43(10):1468–76.  
<https://doi.org/10.1124/dmd.115.065870>.
15. Mohamady A, Shahlaei M, Akbari V, Goicoechea H. C., Jalalvand A. R. Chemometrics-assisted multi-instrumental techniques for investigation of interactions of dapagliflozin with normal and glycated human serum albumin: Application to exploiting second-order advantage for determination of glycated human serum albumin as a biomarker for controlling diabetes. Microchemical Journal. 2021 Aug 1;167.  
<https://doi.org/10.1016/j.microc.2021.106313>.
16. Hashempour S, Shahabadi N, Adewoye A, Murphy B, Rouse C, Salvatore B .A., et al. Binding Studies of AICAR and

- Human Serum Albumin by Spectroscopic, Theoretical, and Computational Methodologies. *Molecules*. 2020 Nov 19;25 (22). <https://doi.org/10.3390/molecules25225410>.
17. Tabassum S, Al-Asbahy W. M., Afzal M, Arjmand F. Synthesis, characterization and interaction studies of copper based drug with Human Serum Albumin (HSA): Spectroscopic and molecular docking investigations. *J Photochem Photobiol B*. 2012 Sep 3;114:132–9. <https://doi.org/10.1016/j.jphotobiol.2012.05.021>.
  18. Ganorkar K, Mukherjee S, Singh P, Ghosh S. K. Stabilization of a potential anticancer thiosemicarbazone derivative in Sudlow site I of human serum albumin: In vitro spectroscopy coupled with molecular dynamics simulation. *Biophys Chem*. 2021 Feb 1;269. <https://doi.org/10.1016/j.bpc.2020.106509>.
  19. Sekowski S, Olchowik-Grabarek E, Wieckowska W, Veiko A, Oldak L, Gorodkiewicz E, et al. Spectroscopic, Zeta-potential and Surface Plasmon Resonance analysis of interaction between potential anti-HIV tannins with different flexibility and human serum albumin. *Colloids Surf B Biointerfaces*. 2020 Oct 1;194. <https://doi.org/10.1016/j.colsurfb.2020.111175>.
  20. Sun X, Bi S, Wu J, Zhao R, Shao D, Song Z. Multispectral and molecular docking investigations on the interaction of primethamine/trimethoprim with BSA/HSA. Vol. 38, *Journal of Biomolecular Structure and Dynamics*. Taylor and Francis Ltd.; 2020. pp. 934–42. <https://doi.org/10.1080/07391102.2019.1588785>.
  21. Amir M, Qureshi M.A., Javed S. Biomolecular interactions and binding dynamics of tyrosine kinase inhibitor erdafitinib, with human serum albumin. *J Biomol Struct Dyn*. 2021;39(11):3934–47. <https://doi.org/10.1080/07391102.2020.1772880>.
  22. MacIązek-Jurczyk M, Sułkowska A, Równicka-Zubik J. Alteration of methotrexate binding to human serum albumin induced by oxidative stress. Spectroscopic comparative study. *Spectrochim Acta A Mol Biomol Spectrosc*. 2016 Jan 5;152:537–50. <https://doi.org/10.1016/j.saa.2014.12.113>.
  23. Fan Y, Zhang S, Wang Q, Li J, Fan H, Shan D. Investigation of the interaction of pepsin with ionic liquids by using fluorescence spectroscopy. *Appl Spectrosc*. 2013 Jun;67(6):648–55. <https://doi.org/10.1366/12-06793>.
  24. Suryawanshi V. D., Anbhule P.V., Gore A. H., Patil S. R., Kolekar G. B. A spectral deciphering the perturbation of model transporter protein (HSA) by antibacterial pyrimidine derivative: Pharmacokinetic and biophysical insights. *J Photochem Photobiol B*. 2013 Jan 5;118:1–8. <https://doi.org/10.1016/j.jphotobiol.2012.09.010>.
  25. Atarodi Shahri P, Sharifi Rad A, Beigoli S, Saberi M.R, Chamani J. Human serum albumin–amlodipine binding studied by multi-spectroscopic, zeta-potential, and molecular modeling techniques. *Journal of the Iranian Chemical Society*. 2018 Jan 1;15(1):223–43. <https://doi.org/10.1007/s13738-017-1226-6>.
  26. Kandandapani S, Kabir M. Z., Ridzwan N. F. W., Mohamad S. B., Tayyab S. Biomolecular interaction mechanism of an anticancer drug, pazopanib with human serum albumin: a multi-spectroscopic and computational approach. *J Biomol Struct Dyn*. 2022;40(18):8312–23. <https://doi.org/10.1080/07391102.2021.1911850>.

27. Kabir M.Z., Ghani H, Mohamad S.B., Alias Z, Tayyab S. Interactive association between RhoA transcriptional signaling inhibitor, CCG1423 and human serum albumin: Biophysical and in silico studies. *J Biomol Struct Dyn*. 2018 Jul 27;36(10):2495–507.  
<https://doi.org/10.1080/07391102.2017.1360207>.
28. Amani N, Reza Saberi M, Khan Chamani J. Investigation by Fluorescence Spectroscopy, Resonance Rayleigh Scatter-ing and Zeta Potential Approaches of the Separate and Simultaneous Binding Effect of Paclitaxel and Estradiol with Human Serum Albumin. Vol. 18, *Protein & Peptide Letters*. 2011.  
<https://doi.org/10.2174/092986611796011473>.
29. Abdollahpour N, Soheili V, Saberi M. R., Chamani J. Investigation of the Interaction Between Human Serum Albumin and Two Drugs as Binary and Ternary Systems. *Eur J Drug Metab Pharmacokinet*. 2016 Dec 1;41(6):705–21.  
<https://doi.org/10.1007/s13318-015-0297-y>.
30. Zhang S, Chen X, Ding S, Lei Q, Fang W. Unfolding of human serum albumin by gemini and single-chain surfactants: A comparative study. *Colloids Surf A Physicochem Eng Asp*. 2016 Apr 20;495:30–8.  
<https://doi.org/10.1016/j.colsurfa.2016.01.051>.
31. Salo-Ahen O. M. H, Alanko I, Bhadane R, Alexandre A. M, Honorato R. V, Hossain S, et al. Molecular dynamics simulations in drug discovery and pharmaceutical development. Vol. 9, *Processes*. MDPI AG; 2021. pp. 1–63.  
<https://doi.org/10.3390/pr9010071>.